https://doi.org/10.29227/IM-2025-02-63 Received: 12 Jun 2025, Accepted: 19 Aug 2025, Published: 20 Oct 2025

Challenges in Estimating Long-Term Insar-Derived Land Subsidence in The Mekong Delta, Vietnam

Artur GUZY[1,*], Wojciech WITKOWSKI[1], Magdalena ŁUCKA[1], Sebastian WALCZAK[1], Pietro TEATINI[2], Philip MINDERHOUD[3]

[1] AGH University of Krakow, Faculty of Geo-Data Science, Geodesy and Environmental Engineering, Krakow, Poland
[2] University of Padova, Department of Civil, Environmental and Architectural Engineering, Padova, Italy
[3] Wageningen University and Research, Soil Geography and Landscape Group, Wageningen, The Netherlands

[*]*Corresponding author: aguzy@agh.edu.pl*

Abstract: *The Mekong Delta in Vietnam is a low-lying, densely populated, and agriculturally important region, making it highly vulnerable to subsidence and sea-level rise. Recent years have seen accelerated subsidence, reaching several centimeters per year, primarily due to intensive groundwater pumping. Previous large-scale InSAR studies have been limited to short timeframes, applied linear assumptions and simplified LOS-to-vertical projections, potentially misrepresenting actual subsidence dynamics.*
In this study, we assessed the feasibility of long-term (2015-2023) subsidence monitoring using Sentinel-1 InSAR, processing a total of 708 descending-mode images with Persistent Scatterer (PS) InSAR and Small Baseline Subset (SBAS) InSAR. Unlike earlier work, our analysis explicitly addresses the challenges of processing large datasets in a coherence-limited delta environment and provides the first systematic comparison of PS and SBAS performance over an eight-year period.
We show that while PS InSAR identified ~564,000 points, primarily in stable urban areas, it largely failed in non-urbanised regions. In contrast, SBAS InSAR yielded ~1,200,000 coherent points, with superior sensitivity to spatially variable subsidence across the delta. By linking InSAR point densities to land cover classes, we further demonstrate that SBAS is particularly effective in vegetated and agricultural areas, whereas PS points remain concentrated in built-up zones. These findings demonstrate that SBAS InSAR is more robust for delta-wide, long-term monitoring.
Given the absence of in-situ validation over the studied period (permanent GNSS stations, levelling benchmarks, extensometers), InSAR currently remains the only comprehensive method for tracking deformation across the Mekong Delta. Our findings establish both the feasibility and the methodological requirements for reliable long-term InSAR-based monitoring in subsiding deltas, and highlight the need for future integration with independent ground-based measurements.

Keywords: *land subsidence; groundwater pumping; relative sea-level rise; InSAR; Mekong Delta*

1. Introduction

Overexploitation of groundwater, causing a significant drop in hydraulic head and resulting in aquifer system compaction, is a primary driver of land subsidence worldwide (Guzy & Malinowska, 2020; Hasan et al., 2023; Shirzaei et al., 2021). This process is particularly problematic in low-lying deltas, where land typically lies less than one meter above sea level (Becker et al., 2024; Small et al., 2018). These densely populated regions are important to global agriculture and economies (Schneider & Asch, 2020; Van Engelen et al., 2022) but are increasingly threatened by relative sea-level rise (rSLR) (Nienhuis et al., 2023). While global sea-level rise is mainly driven by climate change, the dominant component of rSLR in deltas is often land subsidence due to human activities, especially excessive groundwater pumping (Herrera-García, Ezquerro, Tomas, et al., 2021).

Accelerated subsidence in coastal zones leads to increased flood risks, infrastructure damage, loss of agricultural land, salinisation, and, in extreme cases, complete land loss. Current projections estimate a global sea-level rise of 0.61-1.10 m by 2100, which, when combined with subsidence, could be devastating for deltaic communities (Fox-Kemper et al., 2021). Mitigating these impacts requires a thorough understanding of subsidence processes and the development of improved tools for monitoring and prediction.

Interferometric Synthetic Aperture Radar (InSAR) is one of the most widely used methods for measuring subsidence, offering high-resolution observations over large areas (Berardino et al., 2002; Ferretti et al., 2001; Herrera-García, Ezquerro, Tomás, et al., 2021; Raspini et al., 2022). When combined

with numerical models, InSAR helps characterise aquifer system compaction and assess the impact of groundwater pumping. However, as InSAR datasets grow in size and temporal coverage, new challenges in data processing and interpretation emerge.

Most InSAR-based subsidence studies focus on short timeframes, during which standard Persistent Scatterer (PS) and Small Baseline Subset (SBAS) InSAR techniques provide good spatial coverage and high coherence. However, extending this analysis to longer periods leads to increased signal decorrelation due to vegetation, atmospheric effects, and land cover changes over time (Guo et al., 2024; Shirzaei et al., 2021; Xue et al., 2020; Zhao et al., 2019).

In this study, we focus on the Mekong Delta in Vietnam (MKD), one of the most vulnerable and rapidly subsiding delta regions in the world. We first review previous InSAR-based subsidence assessments in the delta, identifying their limitations in spatial coverage, temporal extent, and methodological consistency. We then present long-term analysis using Sentinel-1 data that we processed using PS and SBAS InSAR. We emphasise selected technical challenges in InSAR data processing, including coherence management, coregistration strategies, multi-looking optimisation, and data handling over large spatial and temporal domains. Our objective is to test and evaluate the performance of different InSAR configurations to establish a robust methodology for long-term subsidence monitoring in deltaic environments.

2. Study Area

2.1. Mekong Delta: Main Characteristics, Subsidence Drivers and Modelling Approaches

The MKD is the third-largest delta in the world and home to approximately 18 million people (Fig. 1A) (*General Statistics Office of Vietnam*, 2023). Apart from being densely populated, with Ho Chi Minh City, a sinking megacity (Thao et al., 2024) located in the adjacent and geologically intertwined Saigon River Delta, the MKD holds high agricultural and economic importance. The area is situated at a low elevation, averaging 0.8 m above local sea level (Minderhoud et al., 2019). The region faces growing pressures from sea-level rise (Dang et al., 2022), a declining fluvial sediment supply (Bussi et al., 2021), natural shallow compaction (Baldan et al., 2025; Zoccarato et al., 2018), and accelerated subsidence driven by excessive groundwater pumping (Erban et al., 2014; Minderhoud et al., 2017, 2018). At present, it experiences substantial subsidence, with an average delta-wide rate exceeding 10 mm/year and localised rates as high as 70 mm per year (Dörr et al., 2024). This accelerated subsidence, contributing to rSLR, increases the vulnerability of the MKD to various geohazards, including storm surges (Chen et al., 2024), coastal erosion (Ty et al., 2024), salinization (Duc Tran et al., 2024), infrastructure damage (de Wit et al., 2021), and seasonal flooding (Van et al., 2024).

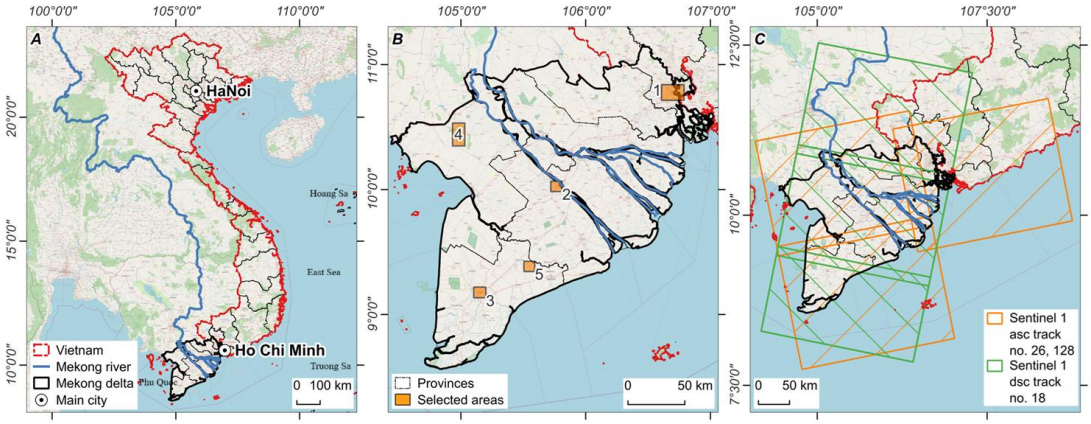

Fig. 1. (A) Location of the MKD within Vietnam; (B) Administrative divisions of the MKD and selected areas used for coherence analysis; (C) Spatial coverage of Sentinel-1 radar acquisitions in ascending and descending modes over the MKD

Subsidence in the MKD results from a combination of natural processes and human activity, occurring at different depths in the subsurface (de Wit et al., 2021). The two main causes are: (1) deep subsidence due to groundwater withdrawal from pre-Holocene aquifers (de Wit et al., 2021; Minderhoud et al., 2017; Minderhoud, Middelkoop, et al., 2020); and (2) shallow subsidence caused by the natural (auto) compaction of Holocene sediments (Baldan et al., 2025; Zoccarato et al., 2018).

To address this, two major modelling frameworks were recently developed. The first one focuses on deep aquifer system compaction, using a 3-D groundwater model developed in the iMOD environment (Minderhoud et al., 2017; Minderhoud, Middelkoop, et al., 2020). This model simulates both groundwater

flow and vertical land movement across the entire MKD, using extensive hydrogeological, geological, and geotechnical datasets. The model includes 15 layers, representing the subsurface with a horizontal resolution of 1 km². A 1-D compaction module (SUB-CR) was used to simulate aquifer system compaction from 1991 to 2020 (Minderhoud et al., 2017), and it has since been extended to project future scenarios to 2100 (Minderhoud, Middelkoop, et al., 2020)

The second modelling effort targets the natural compaction of Holocene sediments, using a custom-built numerical model (NATSUB-3D) that couples shallow lithology, groundwater flow, and geomechanical behaviour. This approach uses lithological bore logs, geochronological data, and spatial interpolation to simulate natural sedimentation and resulting aquifer system compaction over the past ~4000 years (Baldan et al., 2025; Zoccarato et al., 2018).

Together, these models help to distinguish natural and anthropogenic contributions to subsidence in the MKD and provide a foundation for planning mitigation strategies in the region, although research efforts are still ongoing to enhance these modelling frameworks (Guzy et al., 2023; Minderhoud et al., 2023).

2.2. Previous InSAR-based Subsidence Estimates in the Mekong Delta

The application of InSAR in the MKD has significantly advanced over the past decade, providing new insights into the magnitude and spatial distribution of subsidence. Below, we summarise the three most comprehensive InSAR-based subsidence assessments conducted for the delta (Fig. 2).

2.2.1. 2006-2010: First delta-wide InSAR assessment using L-band ALOS PALSAR

The first large-scale InSAR analysis of the MKD was performed using ALOS-1 PALSAR L-band data acquired between 2006 and 2010 (Erban et al., 2014). From 259 acquired images covering most of the delta (with revisit intervals of ~90 days), 121 scenes were selected to create 78 interferograms, grouped into nine stacks (5-12 interferograms each, average of 9), using the interferometric stack method. Only annual interferograms (1 year ± 3 days) were used to minimise the influence of seasonal variability. This approach significantly reduced the temporal resolution but allowed clearer estimates of long-term trends.

Despite limitations, including limited spatial coverage in the southern and coastal delta (due to insufficient acquisitions) and the use of a single ascending geometry, the study successfully estimated subsidence rates of 10-40 mm/year (Fig. 2A). The authors found strong agreement between InSAR-derived rates and compaction estimates from borehole-based hydrogeological models. However, displacements were simplified by projecting LOS (Line of Sight) to vertical, assuming exclusively vertical motion.

The authors emphasised the L-band's advantage in coherence retrieval over vegetated and intermittently flooded areas (e.g., agricultural fields). They also noted that reliable scatterers included infrastructure such as roads and buildings. Despite these successes, the spatial coverage did not extend to low-reflectivity zones in the delta's south and some near-coastal regions.

2.2.2. 2014-2019: C-band Sentinel-1 with PSI

Under the Copernicus Emergency Management Service, the second major InSAR-based subsidence monitoring campaign was conducted by GISAT between November 2014 and January 2019, using Sentinel-1 C-band SAR imagery (European Commission Joint Research Centre (JRC), 2018). This study processed images from descending track 18 (main dataset: 23.11.2014-31.01.2019) and ascending track 26 (validation only: 13.03.2017-26.01.2019) using PS InSAR. The master images were selected from 25.10.2016 (descending) and 01.04.2018 (ascending), with maximum temporal baselines of approximately 700-800 days in each direction.

The spatial extent of the analysis was ~47,800 km^2, excluding regions experiencing high subsidence rates such as Ho Chi Minh City and the southernmost coastal tip of the delta. While no explicit statistics were provided on point density or the total number of PSs, the authors reported subsidence rates of up to 50 mm/year, with substantial variability between urbanised and agricultural areas (Fig. 2B).

The study noted that urban zones exhibited the highest subsidence rates, likely influenced by building loads and deep foundation effects (Minderhoud, Hlavacova, et al., 2020). Some coastal areas also showed signs of significant displacement, though this was flagged for future investigation. Atmospheric artefacts posed challenges, particularly in flood-prone and vegetated areas. Although standard corrections were applied, the authors noted that some regions may still be affected, reducing reliability. As with Erban et al., LOS-to-vertical projection was applied, again assuming purely vertical motion.

https://doi.org/10.29227/IM-2025-02-63 Received: 12 Jun 2025, Accepted: 19 Aug 2025, Published: 20 Oct 2025

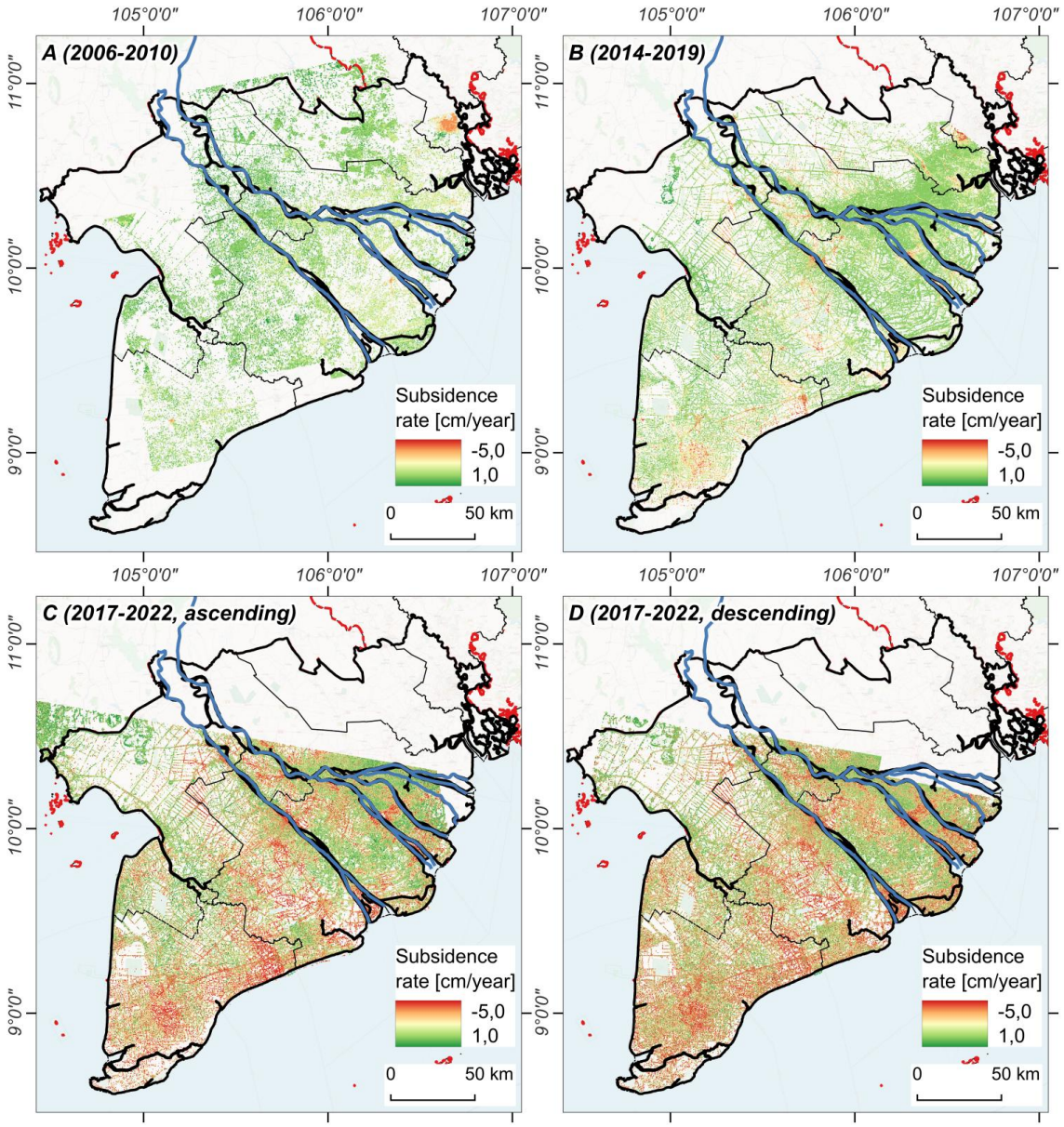

Fig. 2. InSAR-based land subsidence estimates in the MKD: (A) 2006-2010 (Erban et al., 2014); (B) 2014-2019 (European Commission Joint Research Centre (JRC), 2018); (C) 2017-2022: ascending geometry; (C) 2017-2022: ascending and (D) 2017-2022: descending geometry (Dörr et al., 2024)

2.2.3. 2017-2022: High-density PS with dual-geometry and TPS analysis

The most recent and technically advanced assessment covered the period April 2017 to April 2022 using Sentinel-1 imagery from both descending (277 scenes, ~7-day intervals) and ascending (115 scenes, ~16-day intervals) orbits (Dörr et al., 2024). A total of 392 radar images were processed using an enhanced PS InSAR workflow, which included both PS and Temporary Persistent Scatterers (TPS), scatterers with high coherence retained only during parts of the time series, which are especially valuable in dynamic or vegetated zones.

This approach resulted in over 7.1 million observation points in the descending track (including 1.5 million PS and 5.6 million TPS) and 5.2 million points in the ascending track (with 2.4 million PS and 2.8 million TPS), making it the densest InSAR point dataset published for the MKD to date. The study also applied a spatially correlated noise correction, improving the precision of displacement fields.

Subsidence rates exceeded 70 mm/year in some urban areas, and the analysis revealed clear temporal nonlinearities in displacement patterns (Fig. 2C, D). A key innovation was the use of deep-piled bridges as stable reference points, improving accuracy and reducing bias in subsidence estimates. Despite these advancements, the study again assumed exclusively vertical motion by converting LOS displacements to vertical. Reliability flags were assigned to each PS point to identify areas affected by unwrapping errors or inconsistencies between geometries.

In general, the three InSAR-based assessments indicate accelerating rates of subsidence and an increasing spatial extent of affected areas across the MKD. However, each study adopted a different referencing approach for land subsidence estimation, which complicates the direct comparison of their results. In addition to this methodological inconsistency, the studies share common limitations: (1) relatively short observation periods (≤4 years), insufficient to capture longer-term trends; (2) assumption of linear deformation, which neglects nonlinear behavior of aquifer compaction; (3) assumption of purely vertical motion by converting LOS displacements to vertical, which may misrepresent true 3D land movement; and (4) limited spatial coverage, particularly in vegetated, flooded, and low-reflectivity coastal zones.

3. Materials and Methods

3.1. Sentinel-1 Data Availability for the Mekong Delta

The MKD has been continuously monitored by the Sentinel-1 satellites under the Copernicus programme of the European Space Agency since 2014. SAR images are available in two orbit geometries (Fig. 1C). Between 2015 and 2023, a total of 758 descending-mode SAR acquisitions from track 18 were available for the region, with a revisit interval of 12 days, corresponding to ~3,0 TB of raw data. In ascending geometry, 619 images from tracks 26 and 128 were also accessible, acquired at 12-day intervals and resulting in ~2.8 TB. However, the ascending-mode dataset contains a temporal gap in coverage during 2015-2016, which restricts joint analysis over the 2015-2023 period.

Due to this temporal inconsistency and the large data volume, only descending-mode data were used for the long-term analysis presented in this study. To cover the whole MKD, images were collected for three different frames in track 18, resulting in approx. 250 images per frame. Because of inconsistency in the number of bursts or their spatial overlap between images, some acquisitions were removed. The final working dataset comprises a total of 708 images, with 236 acquisitions per frame.

3.2. InSAR Processing Techniques

Two widely used InSAR time series techniques were applied: (1) PS InSAR and (2) SBAS InSAR.

PS InSAR detects coherent, radar-reflective targets, known as PSs, that remain stable over extended periods. This method is well-suited for urban and built-up environments, where stable reflectors are present. It relies on selecting a single master image to which all other acquisitions are coregistered. However, as the temporal baseline increases, coherence often decreases, which limits the number of stable points, particularly in vegetated or agricultural areas (Crosetto et al., 2016; Ferretti et al., 2001).

SBAS InSAR was used as a complementary approach due to its greater suitability for areas with moderate or low temporal coherence. It relies on constructing interferograms with short temporal and spatial baselines, building a redundant network of interferograms. This helps to mitigate decorrelation and improves phase unwrapping accuracy. Unlike PS InSAR, SBAS does not depend on a single master image and is particularly effective in dynamic or vegetated landscapes (Berardino et al., 2002; Li et al., 2022).

In addition to the standard coregistration method, we tested a stacked coregistration approach, where images are iteratively coregistered to their closest temporal neighbours. The process starts with the image closest in time to the master and builds a sequence in which each newly aligned image serves as the reference for the next. Although more computationally intensive, this method may help preserve coherence and improve point density in challenging environments.

3.3. Long-Term Analysis for 2015-2023

For the long-term analysis, the master image from February 6, 2019, was used to generate 708 interferograms for PS InSAR processing (Fig. 3A). SBAS analysis was carried out in parallel using the same dataset and processing parameters to generate 1133 interferograms (Fig. 3B). The original SLC product has a pixel spacing of 2.3 m in slant-range and 14.1 m in azimuth, corresponding to a ground pixel size of ~3 m×16 m. Since processing full-resolution InSAR data is computationally demanding, we tested different Multi-Looking (ML) configurations to reduce noise. A moderate ML factor of 10×2 was adopted as a compromise between spatial detail and computational efficiency, resulting in a ground pixel size of ~30 m.

The objective of this analysis was to evaluate the feasibility and performance of both methods in capturing long-term subsidence across the coherence-limited environment of the MKD. Therefore, no atmospheric filtering or assumption of nonlinear deformation was applied at this stage to isolate the algorithmic behaviour and processing characteristics of each technique. All InSAR data processing was performed using the GAMMA software package (GAMMA Remote Sensing, 2024).

https://doi.org/10.29227/IM-2025-02-63 Received: 12 Jun 2025, Accepted: 19 Aug 2025, Published: 20 Oct 2025

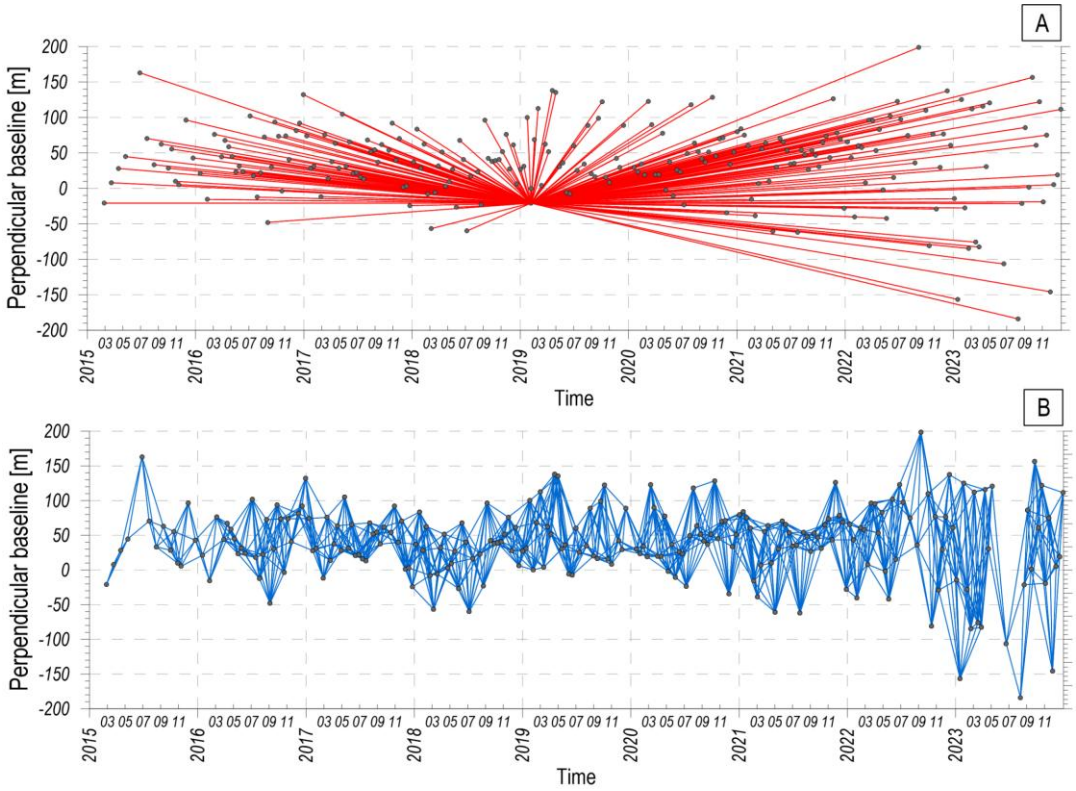

Fig. 3. Distribution of perpendicular and temporal baseline of radar images processed with: PS InSAR (A) and SBAS InSAR (B)

4. Results and Discussion

The long-term InSAR time series encountered several challenges, primarily related to coherence loss and processing complexity. Although the single images exhibited good amplitude quality, the extended temporal baseline in the PS InSAR analysis significantly reduced coherence. Comparisons of coherence and phase images for short (12-day) and long (4-year) temporal baselines confirmed the expected degradation in data quality over time (Fig. 4).

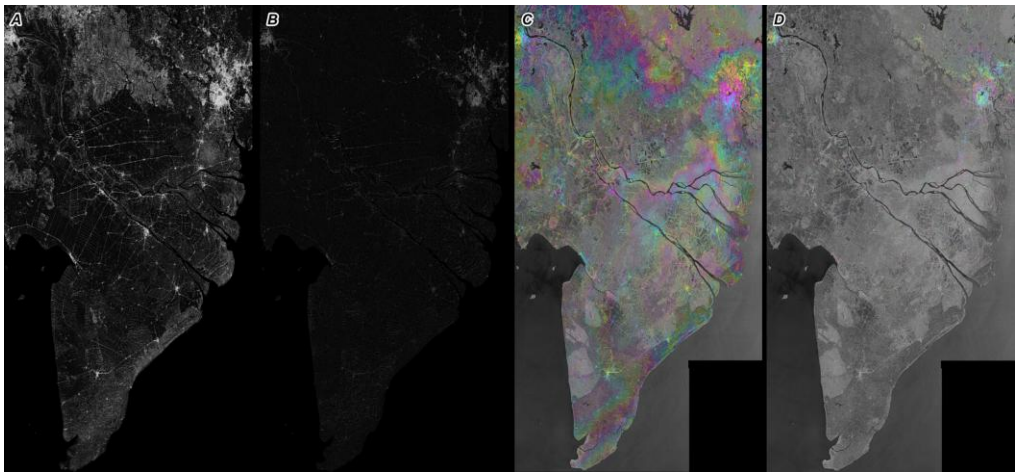

Fig. 4. Radar interferogram coherence and phase example for 12-days (A, C) and 4-years (B, D) time base.

To evaluate the spatial and temporal coherence distribution across MKD, we selected five representative subregions (Fig. 1B). These areas reflect different environmental and land use characteristics: (Area 1) the highly urbanized zone around Ho Chi Minh City; (Areas 2 and 3) moderately urbanized regions around Can Tho and Ca Mau, respectively; (Area 4) (Area 5) a densely vegetated agricultural area near Tri Ton, in proximity to rock outcrops, and (Area 5) a low-vegetation agricultural zone northwest of Bac Lieu.

In the PS InSAR analysis, a significant drop in coherence was observed with increasing temporal baseline across all selected areas (Fig. 5). High coherence values were maintained only for interferograms

with short temporal baselines (up to 2-3 months), followed by a rapid decline for longer periods (Fig. 3A).

By contrast, SBAS InSAR showed consistently better coherence performance (Fig. 6). Due to the constrained temporal (≤48 days) and perpendicular (≤250 m) baselines used in interferogram selection (Fig. 3B), coherence remained relatively stable across the entire period in all five test areas. Minor fluctuations observed in coherence were mainly seasonal and could not be fully mitigated in long-time series analyses.

These differences in coherence impacted the number of detected PS points. For PS InSAR, the difference in point count between the normal and stacked coregistration approaches was marginal, namely ~562,000 vs. ~564,000 points, suggesting limited benefit of the more complex algorithm in low-coherence conditions. In contrast, SBAS InSAR produced substantially higher point densities: ~900,000 points for the normal coregistration and ~1,200,00 million for the stacked approach.

Analysis of point densities across the five selected areas further confirmed this trend (Fig. 7). At the delta-wide scale, PS InSAR resulted in an average point density of ~13.7 points/km^2, whereas SBAS InSAR achieved ~22.4 points/km^2. The highest densities were observed in the urban area of Ho Chi Minh City, with 25.3 (PS) and 277.8 (SBAS) points/km^2. In moderately urbanised areas, such as Ca Mau and Can Tho, PS InSAR detected 6.6 and 2.7 points/km², respectively, while SBAS InSAR achieved significantly better results with 125.2 and 64.4 points/km². In agricultural regions with sparse or moderate vegetation cover (Areas 4 and 5), PS InSAR provided very limited coverage, yielding only 1.4 points/km^2 in Area 5. SBAS InSAR, though still affected by signal decorrelation, maintained a measurable density of ~10.3 points/km^2 in the same area.

To further investigate the relationship between InSAR point density and environmental characteristics, we compared the spatial distribution of PS and SBAS points with land cover classes derived from the ESA World Cover 2021 dataset (Zanaga et al., 2022). This comparison (Fig. 7C) confirms that SBAS InSAR achieves higher coverage in cropland and vegetated areas, whereas PS InSAR points are predominantly concentrated in built-up zones. This difference reflects the methodological capacity of SBAS to detect distributed scatterers (DS), which are more abundant in non-urban environments. However, DS points generally have lower signal-to-noise ratios than PS targets in built-up areas, meaning that displacement values derived from SBAS in agricultural zones should be interpreted with caution and require future validation.

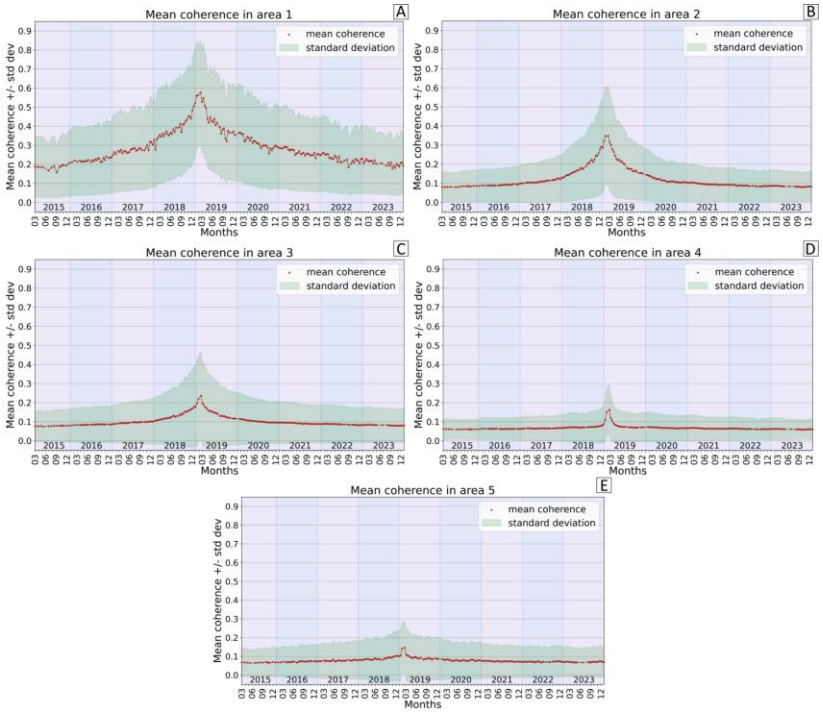

Fig. 5. Mean coherence of interferograms generated using PS InSAR in selected areas 1-5 (A-E). See Fig. 1 for the location of these areas

5. Conclusion

Our results demonstrate that while PS InSAR is valuable for localised and urban-scale applications, it is not well-suited for wide-area, long-term subsidence monitoring in deltaic environments, such as the MKD. Coherence loss in vegetated and hydrologically dynamic regions, combined with long temporal

baselines, significantly limits its effectiveness. In contrast, SBAS InSAR provides better spatial coverage, higher point density, and more robust detection of subsidence across large areas with variable coherence conditions.

These findings should be regarded as preliminary, since our analysis was limited to coherence and point-density metrics, without displacement validation against independent datasets. Nevertheless, they clearly indicate the potential of SBAS InSAR as the more robust approach for delta-wide, long-term monitoring.

Future research should therefore prioritise the use of SBAS InSAR, particularly in combination with advanced coregistration and filtering techniques, for long-term monitoring in delta settings. However, several methodological challenges remain and require further investigation. Firstly, the common assumption of purely vertical motion when projecting LOS into vertical displacement can introduce significant errors, particularly when horizontal displacements are ignored (Brouwer & Hanssen, 2024; Ren & Feng, 2020; Witkowski & Hejmanowski, 2021). Secondly, the widespread use of linear approximation models to represent displacement time series. Secondly, the widespread use of linear approximation models to represent displacement time series neglects nonlinear behaviour that is often observed in geologically dynamic regions (Hussain et al., 2024). Without addressing these issues, InSAR-based models risk producing oversimplified interpretations.

Therefore, to enhance the accuracy and reliability of future delta subsidence assessments, we recommend the following: (1) conducting error assessments related to LOS-to-vertical projection assumptions; (2) developing workflows that accommodate nonlinear time series modelling, especially for multi-year datasets; (3) incorporating horizontal displacement estimation through dual-geometry processing; and (4) integrating independent validation data, such as GNSS, levelling benchmarks, or borehole extensometers. These improvements are required to ensure the robustness of InSAR-based deformation analyses and to support environmental management and policy-making in subsiding delta regions.

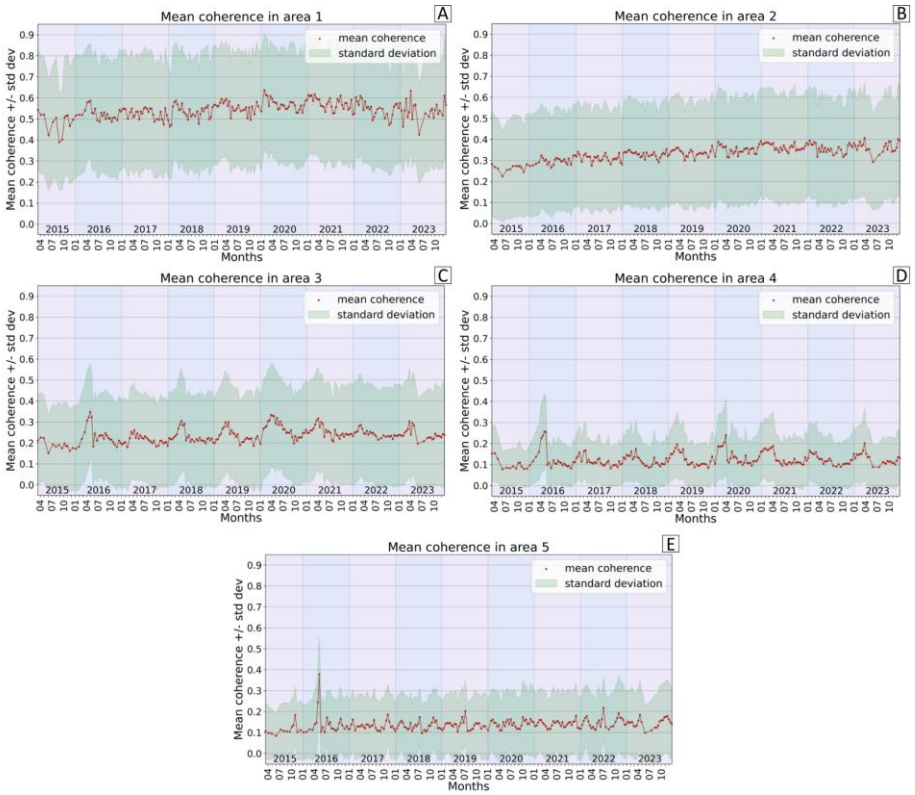

Fig. 6. Mean coherence of interferograms generated using SBAS InSAR in selected areas 1-5 (A-E). See Fig. 1 for the location of these areas

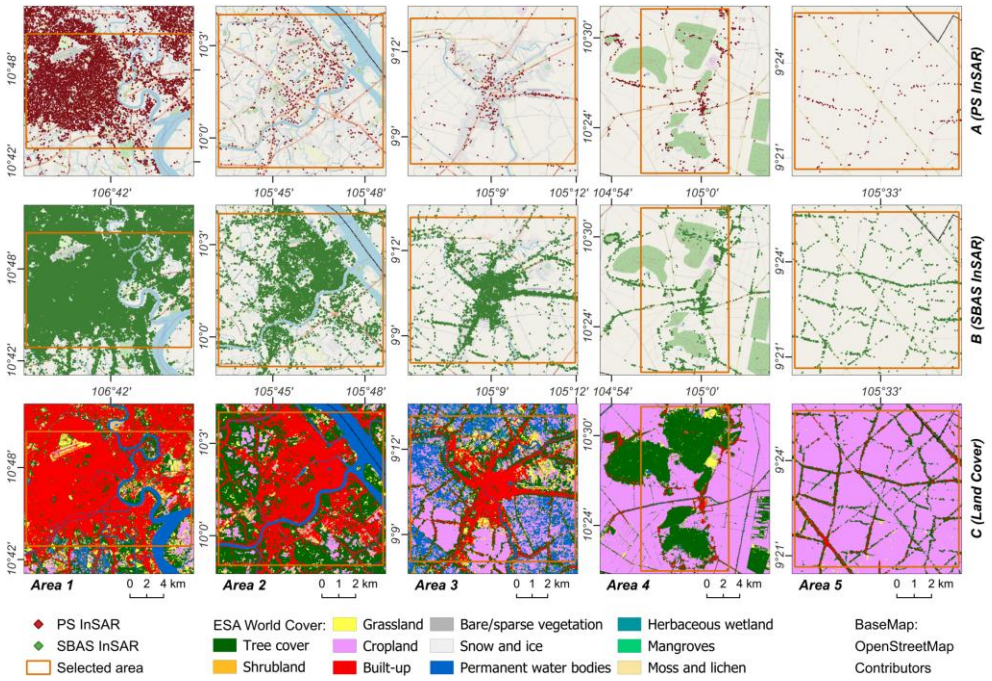

Fig. 7. Differences in point density based on PS InSAR (A) and SBAS InSAR (B) analyses for the period 2015-2023, and land cover (C, (Zanaga et al., 2022)) across selected areas 1-5. See Fig. 1 for the location of the selected areas

Acknowledgment

This research was funded by the National Science Centre, Poland, grant titled "3MAP: Monitoring, Modelling and Mitigation of land subsidence in delta areas", no. 2023/49/B/ST10/01803. For Open Access, the authors have applied a CC-BY public copyright license to any Author Accepted Manuscript (AAM) version arising from this submission. This work contributes to the UNESCO International Initiative on Land Subsidence (www.landsubsidence-unesco.org).

References

Baldan, S., Minderhoud, P. S. J., Xotta, R., Zoccarato, C., & Teatini, P. (2025). Data-driven 3D modelling of long-term Holocene delta evolution and sediment compaction: The Mekong Delta. *Earth Surface Processes and Landforms*, *50*(1), e6046. https://doi.org/10.1002/esp.6046

Becker, M., Seeger, K., Paszkowski, A., Marcos, M., Papa, F., Almar, R., Bates, P., France-Lanord, C., Hossain, M. S., Khan, M. J. U., Karegar, M. A., Karpytchev, M., Long, N., Minderhoud, P. S. J., Neal, J., Nicholls, R. J., & Syvitski, J. (2024). Coastal Flooding in Asian Megadeltas: Recent Advances, Persistent Challenges, and Call for Actions Amidst Local and Global Changes. *Reviews of Geophysics*, *62*(4), e2024RG000846. https://doi.org/10.1029/2024RG000846

Berardino, P., Fornaro, G., Lanari, R., & Sansosti, E. (2002). A new algorithm for surface deformation monitoring based on small baseline differential SAR interferograms. *IEEE Transactions on Geoscience and Remote Sensing*, *40*(11), 2375–2383. https://doi.org/10.1109/TGRS.2002.803792

Brouwer, W. S., & Hanssen, R. F. (2024). Estimating three-dimensional displacements with InSAR: the strapdown approach. *Journal of Geodesy*, *98*(12), 1–15. https://doi.org/10.1007/S00190-024-01918-2/FIGURES/11

Bussi, G., Darby, S. E., Whitehead, P. G., Jin, L., Dadson, S. J., Voepel, H. E., Vasilopoulos, G., Hackney, C. R., Hutton, C., Berchoux, T., Parsons, D. R., & Nicholas, A. (2021). Impact of dams and climate change on suspended sediment flux to the Mekong delta. *Science of The Total Environment*, *755*, 142468. https://doi.org/10.1016/j.scitotenv.2020.142468

Chen, A., Pokhrel, Y., Chen, D., Huang, H., Dai, Z., He, B., Wang, J., Li, J., Wang, H., & Liu, J. (2024). Impact of tropical cyclones and socioeconomic exposure on flood risk distribution in the Mekong Basin. *Communications Earth & Environment*, *5*(1), 704.

https://doi.org/10.1038/s43247-024-01868-9

Crosetto, M., Monserrat, O., Cuevas-González, M., Devanthéry, N., & Crippa, B. (2016). Persistent Scatterer Interferometry: A review. *ISPRS Journal of Photogrammetry and Remote Sensing*, *115*, 78–89. https://doi.org/10.1016/J.ISPRSJPRS.2015.10.011

Dang, A. T. N., Reid, M., & Kumar, L. (2022). Assessing potential impacts of sea level rise on mangrove ecosystems in the Mekong Delta, Vietnam. *Regional Environmental Change*, *22*(2), 70. https://doi.org/10.1007/s10113-022-01925-z

de Wit, K., Lexmond, B. R., Stouthamer, E., Neussner, O., Dörr, N., Schenk, A., & Minderhoud, P. S. J. (2021). Identifying Causes of Urban Differential Subsidence in the Vietnamese Mekong Delta by Combining InSAR and Field Observations. *Remote Sensing*, *13*(2). https://doi.org/10.3390/rs13020189

Dörr, N., Schenk, A., & Hinz, S. (2024). Land Subsidence in the Mekong Delta Derived From Advanced Persistent Scatterer Interferometry With an Infrastructural Reference Network. *IEEE Journal of Selected Topics in Applied Earth Observations and Remote Sensing*, *17*, 12077–12091. https://doi.org/10.1109/JSTARS.2024.3420130

Duc Tran, D., Thi Bich Thuc, P., Park, E., Thi Thanh Hang, P., Ba Man, D., & Wang, J. (2024). Extent of saltwater intrusion and freshwater exploitability in the coastal Vietnamese Mekong Delta assessed by gauging records and numerical simulations. *Journal of Hydrology*, *630*, 130655. https://doi.org/10.1016/j.jhydrol.2024.130655

Erban, L. E., Gorelick, S. M., & Zebker, H. A. (2014). Groundwater extraction, land subsidence, and sea-level rise in the Mekong Delta, Vietnam. *Environmental Research Letters*, *9*(8), 84010. https://doi.org/10.1088/1748-9326/9/8/084010

European Commission Joint Research Centre (JRC). (2018). *Ground subsidence in Mekong delta, Vietnam*. http://data.europa.eu/89h/0f97c8d8-6470-400b-bea3-54ea8fac4294

Ferretti, A., Prati, C., & Rocca, F. (2001). Permanent scatterers in SAR interferometry. *IEEE Transactions on Geoscience and Remote Sensing*, *39*(1), 8–20. https://doi.org/10.1109/36.898661

Fox-Kemper, B., Hewitt, H. T., Xiao, C., Aðalgeirsdóttir, G., Drijfhout, S. S., Edwards, T. L., Golledge, N. R., Hemer, M., Kopp, R. E., Krinner, G., Mix, A., Notz, D., Nowicki, S., Nurhati, I. S., Ruiz, L., Sallée, J.-B., Slangen, A. B. A., & Yu, Y. (2021). Ocean, Cryosphere and Sea Level Change. In V. Masson-Delmotte, P. Zhai, A. Pirani, S. L. Connors, C. Péan, S. Berger, N. Caud, Y. Chen, L. Goldfarb, M. I. Gomis, M. Huang, K. Leitzell, E. Lonnoy, J. B. R. Matthews, T. K. Maycock, T. Waterfield, O. Yelekçi, R. Yu, & B. Zhou (Eds.), *Climate Change 2021: The Physical Science Basis. Contribution of Working Group I to the Sixth Assessment Report of the Intergovernmental Panel on Climate Change* (pp. 1211–1362). Cambridge University Press. https://doi.org/10.1017/9781009157896.011

GAMMA Remote Sensing. (2024). *GAMMA Software: Documentation and References*.

General Statistics Office of Vietnam. (2023). https://www.gso.gov.vn/en/homepage/

Guo, J., Xi, W., Yang, Z., Huang, G., Xiao, B., Jin, T., Hong, W., Gui, F., & Ma, Y. (2024). Study on Optimization Method for InSAR Baseline Considering Changes in Vegetation Coverage. *Sensors 2024, Vol. 24, Page 4783*, *24*(15), 4783. https://doi.org/10.3390/S24154783

Guzy, A., & Malinowska, A. A. (2020). State of the Art and Recent Advancements in the Modelling of Land Subsidence Induced by Groundwater Withdrawal. *Water*, *12*(7). https://doi.org/10.3390/w12072051

Guzy, A., Minderhoud, P., Lexmond, B., Zoccarato, C., & Teatini, P. (2023). Enhancing Predictions of Land Subsidence Induced by the Groundwater Withdrawal in the Mekong Delta, Vietnam. *EGU23*. https://doi.org/10.5194/EGUSPHERE-EGU23-13624

Hasan, M. F., Smith, R., Vajedian, S., Pommerenke, R., & Majumdar, S. (2023). Global land subsidence mapping reveals widespread loss of aquifer storage capacity. *Nature Communications*, *14*(1), 6180. https://doi.org/10.1038/s41467-023-41933-z

Herrera-García, G., Ezquerro, P., Tomas, R., Béjar-Pizarro, M., López-Vinielles, J., Rossi, M., Mateos, R.

M., Carreón-Freyre, D., Lambert, J., Teatini, P., Cabral-Cano, E., Erkens, G., Galloway, D., Hung, W. C., Kakar, N., Sneed, M., Tosi, L., Wang, H., & Ye, S. (2021). Mapping the global threat of land subsidence. *Science*, *371*(6524), 34–36. https://doi.org/10.1126/SCIENCE.ABB8549

Herrera-García, G., Ezquerro, P., Tomás, R., Béjar-Pizarro, M., López-Vinielles, J., Rossi, M., Mateos, R. M., Carreón-Freyre, D., Lambert, J., Teatini, P., Cabral-Cano, E., Erkens, G., Galloway, D., Hung, W.-C., Kakar, N., Sneed, M., Tosi, L., Wang, H., & Ye, S. (2021). Mapping the global threat of land subsidence. *Science*, *371*(6524), 34–36. https://doi.org/10.1126/science.abb8549

Hussain, S., Pan, B., Afzal, Z., Hussain, W., Jianhui, Y., Sajjad, M. M., & Ali, M. (2024). Non-linear ground deformation detection and monitoring using time series InSAR along the coastal urban areas of Pakistan. *Environmental Science and Pollution Research*, *31*(38), 50874–50891. https://doi.org/10.1007/S11356-024-34545-7/FIGURES/12

Li, S., Xu, W., & Li, Z. (2022). Review of the SBAS InSAR Time-series algorithms, applications, and challenges. *Geodesy and Geodynamics*, *13*(2), 114–126. https://doi.org/10.1016/J.GEOG.2021.09.007

Minderhoud, P. S. J., Coumou, L., Erban, L. E., Middelkoop, H., Stouthamer, E., & Addink, E. A. (2018). The relation between land use and subsidence in the Vietnamese Mekong delta. *Science of The Total Environment*, *634*, 715–726. https://doi.org/10.1016/j.scitotenv.2018.03.372

Minderhoud, P. S. J., Coumou, L., Erkens, G., Middelkoop, H., & Stouthamer, E. (2019). Mekong delta much lower than previously assumed in sea-level rise impact assessments. *Nature Communications*, *10*(1), 3847. https://doi.org/10.1038/s41467-019-11602-1

Minderhoud, P. S. J., Erkens, G., Pham, V. H., Bui, V. T., Erban, L., Kooi, H., & Stouthamer, E. (2017). Impacts of 25 years of groundwater extraction on subsidence in the Mekong delta, Vietnam. *Environmental Research Letters*, *12*(6), 64006. https://doi.org/10.1088/1748-9326/aa7146

Minderhoud, P. S. J., Guzy, A., Baldan, S., Xotta, R., Lexmond, B. R., Zoccarato, C., & Teatini, P. (2023). Improving Subsidence Modelling of Different Depth Domains in the Mekong Delta. *Proceedings of the TISOLS Tenth International Symposium on Land Subsidence*, 8.

Minderhoud, P. S. J., Hlavacova, I., Kolomaznik, J., & Neussner, O. (2020). Towards unraveling total subsidence of a mega-delta – the potential of new PS InSAR data for the Mekong delta. *Proceedings of the International Association of Hydrological Sciences*, *382*, 327–332. https://doi.org/10.5194/piahs-382-327-2020

Minderhoud, P. S. J., Middelkoop, H., Erkens, G., & Stouthamer, E. (2020). Groundwater extraction may drown mega-delta: projections of extraction-induced subsidence and elevation of the Mekong delta for the 21st century. *Environmental Research Communications*, *2*(1), 1–14. https://doi.org/10.1088/2515-7620/ab5e21

Nienhuis, J. H., Kim, W., Milne, G. A., Quock, M., Slangen, A. B. A., & Törnqvist, T. E. (2023). River Deltas and Sea-Level Rise. *Annual Review of Earth and Planetary Sciences*, *51*(Volume 51, 2023), 79–104. https://doi.org/10.1146/annurev-earth-031621-093732

Raspini, F., Caleca, F., Del Soldato, M., Festa, D., Confuorto, P., & Bianchini, S. (2022). Review of satellite radar interferometry for subsidence analysis. *Earth-Science Reviews*, *235*, 104239. https://doi.org/10.1016/J.EARSCIREV.2022.104239

Ren, H., & Feng, X. (2020). Calculating vertical deformation using a single InSAR pair based on singular value decomposition in mining areas. *International Journal of Applied Earth Observation and Geoinformation*, *92*, 102115. https://doi.org/10.1016/j.jag.2020.102115

Schneider, P., & Asch, F. (2020). Rice production and food security in Asian mega deltas — A review on characteristics, vulnerabilities and agricultural adaptation options to cope with climate change. *Journal of Agronomy and Crop Science*, *206*(4), 491–503. https://doi.org/10.1111/jac.12415

Shirzaei, M., Freymueller, J., Törnqvist, T. E., Galloway, D. L., Dura, T., & Minderhoud, P. S. J. (2021). Measuring, modelling and projecting coastal land subsidence. *Nature Reviews Earth and Environment*, *2*(1), 40–58. https://doi.org/10.1038/s43017-020-00115-x

Small, C., Sousa, D., Yetman, G., Elvidge, C., & MacManus, K. (2018). Decades of urban growth and development on the Asian megadeltas. *Global and Planetary Change*, *165*, 62–89. https://doi.org/10.1016/j.gloplacha.2018.03.005

Thao, V. T. P., Giang, D. T., & Anh, L. V. (2024). Reliability assessment of land subsidence monitoring results using PSI technique in Ho Chi Minh City, Vietnam. *International Journal of Environmental Studies*, *81*(2), 881–895. https://doi.org/10.1080/00207233.2024.2324623;CTYPE:STRING:JOURNAL

Ty, T. Van, Duy, D. Van, Phat, L. T., Minh, H. V. T., Thanh, N. T., Uyen, N. T. N., & Downes, N. K. (2024). Coastal Erosion Dynamics and Protective Measures in the Vietnamese Mekong Delta. *Journal of Marine Science and Engineering*, *12*(7). https://doi.org/10.3390/jmse12071094

Van, C. T., Thuy, H. T. T., Viet, C. T., Anh, L. N., Van Anh, V. T., & Tran, D. D. (2024). Unveiling flood vulnerability in the Vietnamese Mekong Delta: A case study of an Giang province. *International Journal of Disaster Risk Reduction*, *106*, 104429. https://doi.org/10.1016/j.ijdrr.2024.104429

Van Engelen, J., Oude Essink, G. H. P., & Bierkens, M. F. P. (2022). Sustainability of fresh groundwater resources in fifteen major deltas around the world. *Environmental Research Letters*, *17*(12), 125001. https://doi.org/10.1088/1748-9326/aca16c

Witkowski, W. T., & Hejmanowski, R. (2021). VERTICAL AND HORIZONTAL DISPLACEMENTS ANALYSIS FOR MINING DEFORMATION MODELING. *International Geoscience and Remote Sensing Symposium (IGARSS)*, *2021-July*, 6610–6613. https://doi.org/10.1109/IGARSS47720.2021.9553081

Xue, F., Lv, X., Dou, F., & Yun, Y. (2020). A Review of Time-Series Interferometric SAR Techniques: A Tutorial for Surface Deformation Analysis. *IEEE Geoscience and Remote Sensing Magazine*, *8*(1), 22–42. https://doi.org/10.1109/MGRS.2019.2956165

Zanaga, D., Van De Kerchove, R., Daems, D., De Keersmaecker, W., Brockmann, C., Kirches, G., Wevers, J., Cartus, O., Santoro, M., Fritz, S., Lesiv, M., Herold, M., Tsendbazar, N. E., Xu, P., Ramoino, F., & Arino, O. (2022). *ESA WorldCover 10 m 2021 v200*. Zenodo. https://doi.org/10.5281/zenodo.7254221

Zhao, Q., Ma, G., Wang, Q., Yang, T., Liu, M., Gao, W., Falabella, F., Mastro, P., & Pepe, A. (2019). Generation of long-term InSAR ground displacement time-series through a novel multi-sensor data merging technique: The case study of the Shanghai coastal area. *ISPRS Journal of Photogrammetry and Remote Sensing*, *154*, 10–27. https://doi.org/10.1016/J.ISPRSJPRS.2019.05.005

Zoccarato, C., Minderhoud, P. S. J., & Teatini, P. (2018). The role of sedimentation and natural compaction in a prograding delta: insights from the mega Mekong delta, Vietnam. *Scientific Reports*, *8*(1), 11437. https://doi.org/10.1038/s41598-018-29734-7